Table 1.7.5.1 (*cont.*)

(*c*) SHG (4000–2000 nm).

	$AgGaS_2$	$AgGaSe_2$	$ZnGeP_2$	Tl_3AsSe_3 (TAS)
Crystal class	$\bar{4}2m$	$\bar{4}2m$	$\bar{4}2m$	$3m$
Transparency (μm)	0.5–13	0.78–18	0.74–12	1.3–17
Non-critical λ_{pump} at room temperature (μm)	1.8 and 11.2	3.1 12.8	3.2 10.3	—
Type of phase matching	I	I	I	I
θ (°)	31	52	56	33
φ (°)	—	—	—	—
Effective coefficient d_{eff} (pm V^{-1})	10.4	28	70	68
Angular bandwidth (mrad cm)	3.7	6.0	5.0	4.2
Walk-off angles				
ρ^{ω} (°)	0	0	0.65	0
$\rho^{2\omega}$ (°)	1.2	0.64	0	3.1
Thermal bandwidth (K cm)	50	50	40	5.7 (SHG at 10.6 μm)
Spectral bandwidth (nm cm)	11	22	20	—
Surface optical damage threshold (GW cm^{-2})	0.5 (10 ns bulk)	0.01–0.04 (50 ns, 2 μm) 0.02–0.03 (10 ns at 10.6 μm)	0.05 (25 ns at 2 μm) 1 (2 ns at 10.6 μm)	0.016 (250 ns at 10.6 μm)

exists even if the refractive indices do not vary with the direction of propagation, which would be the case for an interaction involving only ordinary waves during the rotation. The most general expression of the generated harmonic power, *i.e.* $P^{n\omega}(\alpha) = j(\alpha)\sin^2\Psi(\alpha)$, must take into account the angular dependence of all the refractive indices, in particular for the calculation of the coherence length and transmission coefficients (Herman & Hayden, 1995). The effective coefficient is then deduced from the angular spacing of the Maker fringes and from the conversion efficiency at the maxima of oscillation.

A continuous variation of the phase mismatch can also be performed by translating a wedged sample as shown in Fig. 1.7.4.1(*b*) (Perry, 1991). The harmonic power oscillates as a function of the displacement x. In this case, the interacting waves stay collinear and the oscillation is only caused by the variation of the crystal length. Relation (1.7.4.2) is then valid, by considering a variable crystal length $L(x) = x\tan\beta$; $A^{n\omega}$ and $l_c^{n\omega}$ are constant. The space between two maxima of the wedge fringes is $\Delta x_c = 2l_c/\tan\beta$, which allows the determination of l_c. Then the measurement of the harmonic power, $P_{max}^{n\omega}$, generated at a maximum leads to the absolute value of the effective coefficient:

$$|d_{eff}^{n\omega}| = \left\{\frac{P_{max}^{n\omega}}{A^{n\omega}[P^{\omega}(0)]^2 l_c^2}\right\}^{1/2}$$
$$l_c = (\Delta x_c \tan\beta/2). \qquad (1.7.4.3)$$

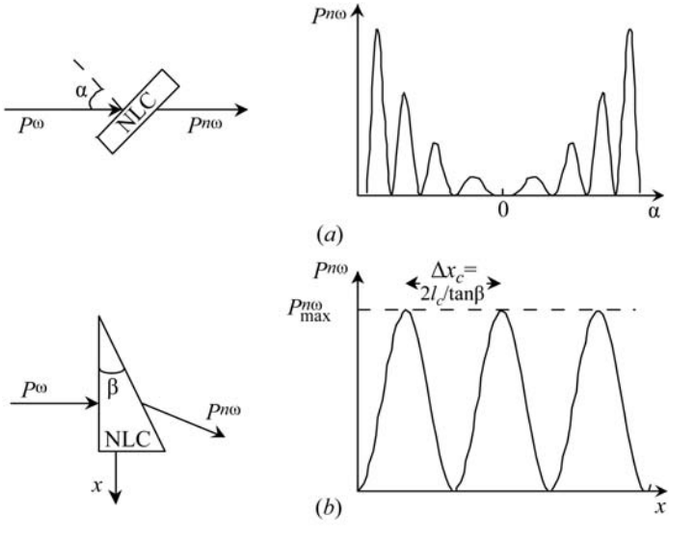

Fig. 1.7.4.1. (*a*) The Maker-fringes technique; (*b*) the wedge-fringes technique.

It is necessary to take into account a multiple reflection factor in the expression of $A^{n\omega}$.

The Maker-fringes and wedge-fringes techniques are essentially used for relative measurements referenced to a standard, usually KH_2PO_4 (KDP) or quartz (α-SiO_2).

1.7.4.2.2. *Phase-matched interaction method*

The use of phase-matched interactions is suitable for absolute and accurate measurements (Eckardt & Byer, 1991; Boulanger, Fève *et al.*, 1994). The sample studied is usually a slab cut in a phase-matching direction. The effective coefficient is determined from the measurement of the conversion efficiency using the theoretical expressions given by (1.7.3.30) and (1.7.3.42) for SHG, and by (1.7.3.80) for THG, according to the validity of the corresponding approximations. Because of phase matching, the generated harmonic power is not weak and it is measurable with very good accuracy, even with a c.w. conversion efficiency.

Recent experiments have been performed in a KTP crystal cut as a sphere (Boulanger *et al.*, 1997, 1998): the absolute magnitudes of the quadratic effective coefficients are measured with an accuracy of 10%, which is comparable with typical experiments on a slab.

For both non-phase-matched and phase-matched techniques, it is important to know the refractive indices and to characterize the spatial, temporal and spectral properties of the pump beam carefully. The considerations developed in Section 1.7.3 about effective coefficients and field tensors allow judicious choices of configurations of polarization and directions of propagation for the determination of the absolute value and relative sign of the independent coefficients of tensors $\chi^{(2)}$ and $\chi^{(3)}$, given in Tables 1.7.2.2 to 1.7.2.5 for the different crystal point groups.

1.7.5. The main nonlinear crystals

Tables 1.7.5.1 and 1.7.5.2 give some characteristics of the main nonlinear crystals. No single nonlinear crystal is the best for all applications, so the different materials must be seen as complementary to each other.

A complete review of mineral crystals is given in Bordui & Fejer (1993). General references for organic crystals may be found, for example, in Chemla & Zyss (1987), Zyss (1994), and Dmitriev *et al.* (1991). Perry (1991) deals with both organic and inorganic materials.

A new generation of materials has been developed since 1995 for the design of new compact all-solid-state laser sources. These optical materials are multifunction crystals, such as $LiNbO_3$:Nd^{3+}, $Ba_2NaNb_5O_{15}$:Nd^{3+}, $CaGd_4(BO_3)_3O$:Nd^{3+} or $YAl_3(BO_3)_4$:Yb^{3+}, for example, in which the laser effect and the nonlinear frequency

Table 1.7.5.2. *Organic and organo-mineral crystals*

Abbreviations for crystals: 5-NU: 5-nitrouracil; MAP: methyl-(2,4-dinitrophenyl)-aminopropanoate; MNA: 2-methyl-4-nitroaniline; POM: 3-methyl-4-nitropyridine-*N*-oxide; NPP: *N*-(4-nitrophenyl)-L-propinol; 2A5NPDP: 2-amino-5-nitropyridine dihydrogen phosphate. OPA, OPO and SROPO are abbreviations for optical parametric amplification, oscillation and single resonant optical parametric oscillator, respectively. 1 e.s.u. = 4.19×10^{-4} m V^{-1}.

Crystal	Space group	Transparency	Refractive index phase matching (PM)	Damage threshold
Urea	$P\bar{4}2_1m$	220 nm to 2 μm	90° type-II PM at 597 nm PM to 238 nm	1.4 GW cm^{-2} at 354.7 nm
5-NU	$P2_12_12_1$	410 nm to 2 μm	$n_b > n_c > n_a$ Types I and II for SHG and SFG ($\omega + 2\omega \rightarrow 3\omega$)	
MAP	$P2_1$	500 nm to 2 μm	$n_x < n_y < n_z$ Non-critical PM: at 1.083 μm (along z); at 1.06 μm (between room temperature and liquid N_2)	>3 GW cm^{-2} at 1.06 μm, 10 ns, 10 Hz >150 MW cm^{-2} at 532 nm, 7 ns, 10 Hz
MNA	Cc	500 nm to 2 μm	$n_x = 2.093$ and $n_y = 2.494$ at 1.06 μm	
POM	$P2_12_12_1$	500 nm to 2 μm	$n_b > n_a > n_c$ Type-I PM tunable from 2 μm to 0.8 μm	∼1 TW cm^{-2} at 610 nm (10 Hz, 100 fs) 2 GW cm^{-2} at 1.06 μm (20 ps) 150 MW cm^{-2} at 0.532 μm (20 ps) 50 MW cm^{-2} at 0.532 μm (10 ns)
NPP	$P2_1$	500 nm to 2 μm	$n_y > n_x > n_z$ $n_x - n_z = 0.78$ at 532 nm Non-critical PM at 1.15 μm $d\theta_{PM}/dT = -0.303$ mrad K^{-1}	10 GW cm^{-2} at 620 nm (100 fs, 10 Hz)
2A5NPDP	$Pna2_1$	0.420 to 1.7 μm	$n_x < n_y < n_z$ $n_z - n_x = 0.158$ at 546 nm $n_z - n_y = 0.152$ at 546 nm Type-II non-critical PM at 1.06 μm at 210 K Type-I ($d_{eff} = 2.25$ pm V^{-1}) PM at 1.34 μm Type-II ($d_{eff} = 4.5$ pm V^{-1}) PM at 1.34 μm $d\theta_{PM}/dT = -0.137$ mrad K^{-1} for type II at 1.34 μm $d\lambda/dT = 0.176$ nm K^{-1} for PM ($295 < T < 343$ K)	
DAST	Cc	700 nm to 2 μm	$n_1(720\text{ nm}) = 2.519$ $n_2(720\text{ nm}) = 1.720$ $n_3(720\text{ nm}) = 1.635$	
2A5NPCl	$P2_1$	410 nm to 1.65 μm	See Horiuchi *et al.* (2002)	

Crystal	Nonlinear coefficients SHG (d_{ij}) and EO (r_{ij})	OPO/OPA	References†
Urea	$d_{14} = 1.4$ pm V^{-1} $r_{41} = 56 \times 10^{-9}$ e.s.u. $r_{63} = 25 \times 10^{-9}$ e.s.u.	SRO $\lambda_p = 354.7$ nm $t_p = 7$ ns Yield: 20.5% Threshold: 45 mW Output: 6 mW at 1.22 μm Tunability: 0.499 to 1.23 μm	(*a*), (*b*), (*c*), (*d*)
5-NU	$d_{14} = d_{25} = d_{36} = 8.7$ pm V^{-1} at 1.06 μm		(*e*)
MAP	$d_{21} = 40 \pm 5 \times 10^{-9}$ e.s.u. $d_{22} = 44 \pm 5 \times 10^{-9}$ e.s.u. $d_{23} = 8.8 \pm 2 \times 10^{-9}$ e.s.u. $d_{25} = -1.3 \pm 2 \times 10^{-9}$ e.s.u.		(*f*)
MNA	$d_{11} = 250$ pm V^{-1} at 1.06 μm $d_{11} = 190$ pm V^{-1} at 1.2 μm $d_{11} = 165$ pm V^{-1} at 1.3 μm $d_{11} = 145$ pm V^{-1} at 1.47 μm $d_{11} = 125$ pm V^{-1} at 1.54 μm $(d_{11}^2/n^3)_{MNA} = 2000(d_{11}^2/n^3)_{LiNbO_3}$ $r_{11} = 67 \pm 25$ pm V^{-1} at 632.8 nm $\frac{1}{2}(n_1^3 r_{11} - n_3^3 r_{31}) = 270 \pm 50$ pm V^{-1}		(*g*), (*h*), (*i*)
POM	$d_{14} = d_{25} = d_{36} = 23 \pm 3$ pm V^{-1} at 1.06 μm $r_{41} = 3.6 \pm 0.6$ pm V^{-1} at 632.8 nm $r_{52} = 5.1 \pm 0.4$ pm V^{-1} at 632.8 nm $r_{63} = 2.6 \pm 0.3$ pm V^{-1} at 632.8 nm	OPA: $G = 10^3$ $\lambda_p = 532$ nm, 10 Hz, 25 ps $I_p = 130$ MW cm^{-2} Infrared input: 5 kW cm^{-2} at degeneracy	(*j*), (*k*), (*l*), (*m*), (*n*)
NPP	$d_{21} = 56.5 \pm 5$ pm V^{-1} at 1.34 μm $d_{22} = 18.7 \pm 2$ pm V^{-1} at 1.34 μm $d_{22} = 128$ pm V^{-1} at 1.06 μm $r_{12} = 25.5$ pm V^{-1} at 632.8 nm $r_{22} = 24$ pm V^{-1} at 632.8 nm $n^3 r_{eff} = 60$ pm V^{-1} at 1.34 μm	OPA: G ≃ 10^4 at degeneracy (1.24 μm); pump: 620 nm, 100 fs, 10 Hz OPO, λ_{pump} tuning: $593 < \lambda_p < 670$ nm, $1000 < \lambda_{i,s} < 1500$ nm OPO, birefringence tuning: $\lambda_p = 670$ nm, $900 < \lambda_{i,s} < 1700$ nm DRO threshold at 670 nm: 0.45 MW cm^{-2}, pump: 2.3 MW cm^{-2} (60 ns, 10 Hz). Yield: 4.5%, IR_{output} 90 μJ	(*m*), (*o*), (*p*), (*q*), (*r*), (*s*)
2A5NPDP	At 1.34 μm: $d_{33} = 12 \pm 1$ pm V^{-1}, $d_{15} = 6 \pm 1$ pm V^{-1} At 1.06 μm: $d_{24} = 1 \pm 0.4$ pm V^{-1}, $d_{15} = 7 \pm 1$ pm V^{-1}	OPA: $\Gamma = 29 \pm 3$ cm^{-1} ($I_p = 30$ GW cm^{-2}); $d_{eff} = 2.6 \pm 0.5$ pm V^{-1}; $\lambda_s = 1.005$ μm, $\lambda_p = 612$ nm OPA: $\Gamma = 19 \pm 3$ cm^{-1}, $G = 10^6$, $\lambda_s = 1$ μm, $\lambda_i = 1.5$ μm, $\lambda_p = 612$ nm OPO: λ_{pump} tuning: $565 < \lambda_p < 590$ nm; $\lambda_s \simeq 1.003$ μm; $1286 < \lambda_i < 1500$ nm SRO: threshold: 6 MW cm^{-2}; $I_p = 37.2$ MW cm^{-2} (7 ns, 10 Hz); yield 3%, IR_{output} 150 μJ	(*r*), (*s*), (*t*), (*u*)

Table 1.7.5.2 (*cont.*)

Crystal	Nonlinear coefficients SHG (d_{ij}) and EO (r_{ij})	OPO/OPA	References†
DAST	d_{11}(1318 nm) = 1010 pm V^{-1} d_{11}(1542 nm) = 290 pm V^{-1} d_{26}(1542 nm) = 39 pm V^{-1} r_{11}(720 nm) = 92 pm V^{-1} r_{11}(1313 nm) = 53 pm V^{-1} r_{11}(1535 nm) = 47 pm V^{-1}	Terahertz generation (difference frequency mixing)	(*v*), (*w*)
2A5NPCl	d_{11} = 9 ± 4 pm V^{-1} d_{12} = 8 ± 3 pm V^{-1} d_{13} = 11 ± 4 pm V^{-1} $d_{\rm eff}$ = 5.1 pm V^{-1} or 9.7 pm V^{-1}		(*x*)

† References: (*a*) Halbout *et al.*, 1979; (*b*) Morrell *et al.*, 1979; (*c*) Donaldson & Tang, 1984; (*d*) Rosker *et al.*, 1985; (*e*) Puccetti *et al.*, 1993; (*f*) Oudar & Hierle, 1977; (*g*) Levine *et al.*, 1979; (*h*) Lipscomb *et al.*, 1981; (*i*) Morita *et al.*, 1988; (*j*) Zyss *et al.*, 1981; (*k*) Sigelle & Hierle, 1981; (*l*) Zyss *et al.*, 1985; (*m*) Ledoux *et al.*, 1987; (*n*) Josse *et al.*, 1988; (*o*) Ledoux *et al.*, 1990; (*p*) Josse *et al.*, 1992; (*q*) Khodja *et al.*, 1995(*b*); (*r*) Khodja, 1995; (*s*) Zyss *et al.*, 1984; (*t*) Kotler *et al.*, 1992; (*u*) Fève *et al.*, 1999; (*v*) Bosshard, 2000; (*w*) Kawase *et al.*, 2000; (*x*) Horiuchi *et al.*, 2002.

conversion occur simultaneously inside the same crystal. An overview of these attractive materials is given in Brenier (2000).

1.7.6. Glossary

μ_0	vacuum magnetic permeability
ε_0	permittivity of free space
c	velocity of light in a vacuum
$\mathbf{P}$	electronic polarization
$\mathbf{P}_n$	nth order electronic polarization
$\mathbf{P}^{\rm NL}$	nonlinear polarization
$\chi^{(n)}$	nth order dielectric susceptibility tensor
ε	dielectric tensor
n	refractive index
n_x, n_y, n_z	principal refractive indices
(x, y, z)	principal axes of the index surface (optical frame)
n_o, n_e	refractive indices of the ordinary and extraordinary eigen modes
T	transmission coefficient
V	half of the angle between optic axes
ω	laser circular frequency
λ	laser wavelength
φ	laser phase
v_g	laser group velocity
$\mathbf{k}$	wavevector
$\mathbf{u}$	unit wavevector
(θ, φ)	spherical coordinates of the wavevector in the optical frame
Π	neutral vibration plane
$\mathbf{E}$	electric field vector
$(\mathbf{e}, E)$	unit vector and amplitude of the electric field
$\mathbf{D}$	dielectric displacement vector
$\mathbf{d}$	unit dielectric displacement vector
$\mathbf{H}$	magnetic field vector
$\mathbf{S}$	Poynting vector
$\mathbf{s}$	unit Poynting vector
W	work done per unit time
(X, Y, Z)	orthonormal wave frame where Z is along the wavevector
ρ	double refraction angle (walk-off angle)
∇	nabla operator
$\otimes$	tensorial product
$\cdot$	tensorial contraction
$\times$	vectorial product
Q^*	complex conjugate of Q
w_0	laser beam waist radius
Z_R	Rayleigh length of the laser beam
τ	laser pulse half duration
f	repetition rate of the pulsed laser
P, $P(t)$	laser instantaneous power
I	instantaneous laser intensity
$\tilde{E}$	total energy per laser pulse
$\tilde{P}$	average laser power
P_c	laser peak power
L	crystal length
$\chi_{\rm eff}$, $d_{\rm eff}$	effective coefficient
$\mathbf{F}^{(n)}$	nth order field tensor
Δk	phase mismatch
$\eta_{\rm SHG}$	conversion efficiency of second harmonic generation
G, h	spatial walk-off attenuation functions

We thank Dr J. P. Fève for his valuable assistance and critical reading of the manuscript.

References

Akhmanov, S. A., Kovrygin, A. I. & Sukhorukov, A. P. (1975). *Treatise in quantum electronics*, edited by H. Rabin & C. L. Tang. New York: Academic Press.

Armstrong, J. A., Bloembergen, N., Ducuing, J. & Pershan, P. (1962). *Interactions between light waves in a nonlinear dielectric. Phys. Rev.* **127**, 1918–1939.

Asaumi, K. (1992). *Second harmonic power of $KTiOPO_4$ with double refraction. Appl. Phys. B*, **54**, 265–270.

Ashkin, A., Boyd, G. D. & Dziedzic, J. M. (1966). *Resonant optical second harmonic generation and mixing. IEEE J. Quantum Electron.* **QE2**, 109–124.

Baumgartner, R. A. & Byer, R. L. (1979). *Optical parametric amplification. IEEE J. Quantum Electron*. **QE15**, 432–444.

Bloembergen, N. (1963). *Some theoretical problems in quantum electronics. Symposium on optical masers*, edited by J. Fox, pp. 13–22. New York: Intersciences Publishers.

Bloembergen, N. (1965). *Nonlinear optics*. New York: Benjamin.

Bordui, P. F. & Fejer, M. M. (1993). *Inorganic crystals for nonlinear optical frequency conversion. Annu. Rev. Mater. Sci.* **23**, 321–379.

Bosshard, C. (2000). *Third order nonlinear optics in polar materials*. In *Nonlinear optical effects and materials*, edited by P. Günter, pp. 7–161. Berlin: Springer Verlag.

Boulanger, B. (1989). *Synthèse en flux et étude des propriétés optiques cristallines linéaires et non linéaires par la méthode de la sphère de $KTiOPO_4$ et des nouveaux composés isotypes et solutions solides de formule générale (K,Rb,Cs)TiO(P,As)O_4.* PhD Dissertation, Université de Nancy I, France.

Boulanger, B. (1994). CNRS–NSF Report, Stanford University.

Boulanger, B., Fejer, M. M., Blachman, R. & Bordui, P. F. (1994). *Study of $KTiOPO_4$ gray-tracking at 1064, 532 and 355 nm. Appl. Phys. Lett.* **65**(19), 2401–2403.

Boulanger, B., Fève, J. P. & Marnier, G. (1993). *Field factor formalism for the study of the tensorial symmetry of the four-wave non linear optical parametric interactions in uniaxial and biaxial crystal classes. Phys. Rev. E*, **48**(6), 4730–4751.